ChemComm

Accepted Manuscript

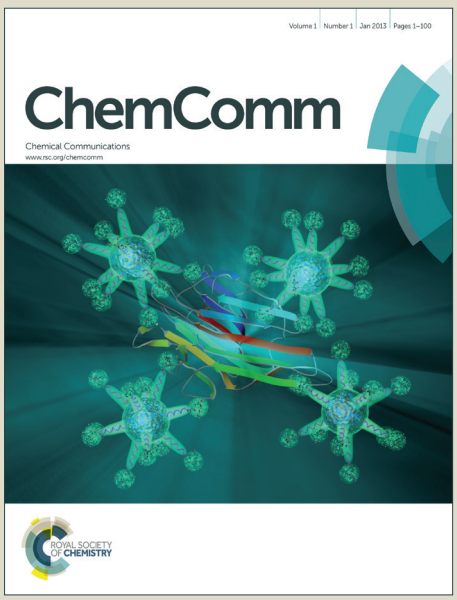

ROYAL SOCIETY OF CHEMISTRY

www.rsc.org/chemcomm

Cite this: DOI: 10.1039/c0xx00000x

www.rsc.org/xxxxxx

COMMUNICATION

A Facile Strategy to Generate Polymeric Nanoparticles for Synergistic Chemo-photodynamic Therapy

Xin Deng, Yan Liang, Xinyu Peng, Ting Su, Song Luo, Jun Cao*, Zhongwei Gu and Bin He*

Received (in XXX, XXX) Xth XXXXXXXXX 20XX, Accepted Xth XXXXXXXXX 20XX

DOI: 10.1039/b000000x

Synergistic therapy is a promising strategy for cancer treatment. A nanoparticle with chemo-photodynamic combination therapy was fabricated via π-π stacking interaction between drug and photosensitizer. It exhibited efficient anticancer activity both *in vitro* and *in vivo*.

Synergistic therapy was considered as a promising strategy for cancer therapy. The nanoparticles with two or more therapeutics targeted to different sites in tumors were more efficiently to induce the apoptosis of cancer cells and inhibit the growth of cancer tissues.[1] The nanoparticles with synergistic chemo-chemo, chemo-SiRNA, chemo-thermal, and chemo-photodynamic therapies were formulated and focused passionately in recent years.[2]

Photodynamic therapy (PDT) is a non-invasive therapeutic mode, it has been widely utilized in the treatment of many diseases. The activation of photosensitizers generated reactive oxygen species (ROS) to cause cell death and tissue destruction.[3] In the combination of chemo and photodynamic therapy, both chemotherapeutics and photosensitizers were co-loaded in nanoparticles and delivered to tumors.[4] However, unavoidable limitations such as low drug loading content and uncontrollable release manner were existed in the co-delivery.[4, 5]

Strategies were developed to improve drug loading content. Many chemotherapeutics have π-π conjugated moieties. The π-π stacking interaction was helpful for drug loading,[6] which was used to absorb massive anticancer drugs on carbon nanotube and graphene.[6, 7] π-π stacking interaction was reported in low molecular weight hydrogels (LMWH) with exciting drug loading content[8] and anticancer efficacy. Polymeric nanoparticles are important carriers, different from carbon nanomaterials and LMWH,[8,9] the encapsulation pattern in drug loading[10] led to poor loading content, although crosslinking and conjugation were attempted to improve drug loading content in polymeric nanoparticles,[11] rare optimistic results were received.

We developed a facile strategy to generate polymeric nanoparticles for synergistic chemo-photodynamic therapy with introducing π-π stacking interaction between anticancer drug and photosensitizer. The photosensitizer was not conjugated to the hydrophobic biodegradable block in polymeric micelles,[12] it was immobilized directly on the hydroxyl group pf methoxy poly(ethylene glycol) (mPEG-Por). Doxorubicin (DOX) was trapped in the self-assembled nanoparticles with π-π stacking interaction to generate high drug loading content.

There were four carboxyl groups in Por, each Por molecule was designed to immobilize one mPEG chain, the received mPEG-Por conjugates were characterized by ^{1}H NMR, MS and GPC. The ^{1}H NMR spectrum of mPEG-Por conjugates with $CDCl_3$ as solvent was presented in Figure 1A, the strong proton signal appeared at δ=3.6 ppm was assigned to the protons of CH_2CH_2O units in mPEG, the chemical environment of protons in OCH_3 and $COOCH_2$ in the two terminals of mPEG was different from other protons in mPEG (δ=3.6 ppm), which was shifted to high field at δ=3.4 ppm for OCH_3 and low field from δ=3.9 to 4.2 ppm for $COOCH_2$. The protons in Por moieties were from δ=7.5 to 9.0 ppm and split into multiple peaks. In the MS spectrum (Figure S1A), two molecule weight peaks at about 2700 and 4600 were found. Although the molar ratio of Pro to mPEG chain was 1:1 in the feeding dose, it was unavoidable to receive a small amount of conjugates with two mPEG chains. This was also demonstrated in GPC (Figure S1B) spectrum. As both conjugates with one or two mPEG chains were amphiphiles, the self-assembly of the mPEG-Por would not be affected by the small quantity of conjugates with two mPEG chains. The proton signals of Por disappeared completely in the ^{1}H NMR spectrum with D_2O as solvent in Figure 1A,[13] revealing the formation of mPEG-Por nanoparticles.

The mean size of blank nanoparticles was 63 nm and that of drug loaded nanoparticles was 115 nm, the particle size was enlarged due to drug encapsulation (Figure 1B). The Zeta potentials varied from -28.4 to -12.8 mV. Both nanoparticles were spherical in TEM and AFM images (Figure 1D, S2) and smaller than DLS results due to the shrinkage in the drying process.[14]

Pyrene fluorescence probe is usually used to test the critical aggregation concentration (CAC) of nanoparticles,[15] but it was not suitable for mPEG-Por nanoparticles as Por disturbed the fluorescence. Here, we used conductivity measurement for CAC testing, which was 11.5 μg/mL (Figure S2A). Porphorin fluorescence probe was also used to measure the CAC. The test mechanism was the same as pyrene fluorescence probe (Figure S2B, S3). The tested CAC was 12.5 μg/mL, which was similar to the result of conductivity measurement. The nanoparticles were found stable in aqueous solution (Figure S4) .

The drug loading content (DLC) and drug encapsulation efficiency (DEE) were 17.9% and 89.3%, which were much higher than other polymeric nanoparticles previously reported[16] due to the π-π stacking interaction between DOX and mPEG-Por nanoparticles.[17] The Fluorescent quenching was used to characterize π-π stacking interaction.[17a, 18] The emission at around

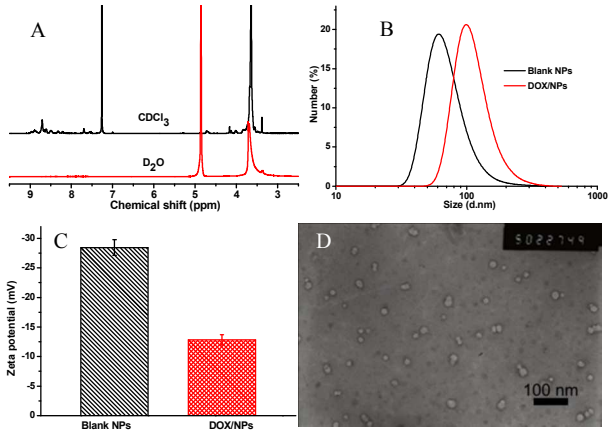

Figure 1. Properties of mPEG-Por nanoparticles, (A) the ^{1}H NMR spectra of mPEG-Por conjugate with $CDCl_3$ and D_2O as solvents; (B) DLS results of blank NPs and DOX loaded NPs; (C) zeta potentials of blank NPs and DOX loaded NPs; (D) TEM image of DOX loaded NPs.

550 nm was the fluorescence of DOX and that at about 650 nm (Figure S5) was the fluorescence of porphyrin in mPEG-Por conjugate.[19] The intensity of prophyrin fluorescence was enhanced and that of DOX was weakened when the concentration of mPEG-Por increased. The increase of prophyrin concentrations not only offset the quenching of prophyrin fluorescence but also strengthened the emission of prophyrin fluorescence greatly (Figure 2A). Keeping the concentration of mPEG-Por stable and increasing the concentration of DOX, the quenching phenominon happened in prophyrin fluorescence band and the intensity of DOX fluorescence was strengthened (Figure 2B). These results clearly revealed the formation of π-π stacking interaction between DOX and mPEG-Por conjugate.

Red shift in UV-vis spectra is another characteristic of π-π stacking interaction.[18, 20] Red shift was observed when the concentration of mPEG-Por was changed from 4 to 200 μg/mL (Figure S6). The UV-vis spectra of mPEG-Por conjugates and self-assembled nanoparticles were tested (Figure 2C), the main absorbance of prophorin and mPEG-Por conjugate was at 512 nm in methanol. The absorbance of the samples with 100 and 200 μm/mL concentrations was at 519 nm, demonstrating the π-π stacking interaction in mPEG-Por nanoparticles.

The fluorescence spectra of drug loaded nanoparticles were tested in methanol and PBS (Figure 2D, S7) to explore the π-π stacking interaction. The intensities of DOX and Por fluorescence in methanol were much stronger than those in PBS, indicating the π-π stacking interaction between DOX and mPEG-Por conjugate. The intensity of Por fluorescence in blank nanoparticles was weaker to that of DOX loaded nanoparticles in methanol due to the emission of DOX in this band partially overlapped the emission of Por in nanoparticles to enhance the intensity.

Methanol was added in the aqueous solution of DOX loaded nanoparticles to destroy the π-π stacking interaction between DOX and nanoparticles (Figure 2E). The quenching of both fluorescence of DOX and Por was weakened, the intensities increased continuously and stabilized when the volume of methanol exceeded 2000 μL to show the destruction of π-π stacking interaction. The drug release profile was similar to that of other polymeric nanoparticles based delivery systems (Figure 2F). About 30 % loaded drugs was fast released in the first 10 h, the release was slow down and 40% drug was released in 50 h.

The cytotoxicity of the nanoparticles was evaluated in three cancer cell lines of HepG2, 4T1 and Hela cells. All the cell viability was higher than 80% to reveal the non-cytoxicity of blank nanoparticles (Figure S8). In the CLSM images, most fluorescence of both DOX and nanoparticles were located in cytoplasm, the intensity for 6 h incubation was stronger (Figure 3A). The quantitative results of cellular uptake tested by flow cytometry showed the same results (Figure 3B). More DOX/NPs were endocytosized in 4T1 cells with higher concentrations (Figure S9). The group of DOX/NPs with laser irradiation (Figure 3C) exhibited the best anticancer activity.

Nanoparticles were passively targeted to cancers via EPR effect.[21] The tumor targeting effect of DOX/NPs was obvious (Figure 4A), strong fluorescence was observed in tumor after DOX/NPs were injected for 0.5 h. The fluorescence in tumor was maintained for 10 h while the fluorescence in other organs was weakened greatly. The fluorescence in tumor was observed after 24 h injection. Further targeting effect of the nanoparticles was investigated via *ex vivo* imaging (Figure S10). The strongest fluorescence in tumor implied the passive targeting effect. The quantitative biodistribution of nanoparticles was showed via the fluorescence intensity of nanoparticles in organs (Figure S10b), the strong fluorescence intensity demonstrated that the nanoparticles were aggregated in tumor.

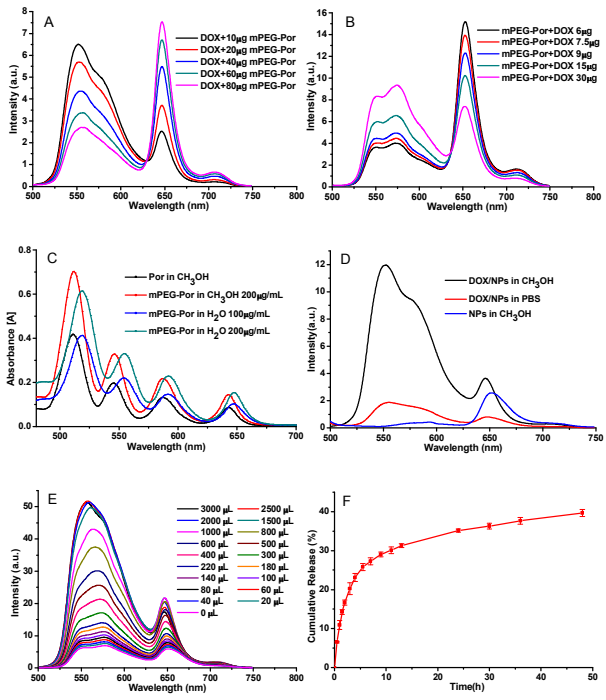

Figure 2. The π-π interaction between mPEG-Por and DOX, (A) fluorescence spectra of mixtures of DOX and mPEG-Por conjugate, DOX 1.5 μg in 1 mL DMSO; (B) fluorescence spectra of the mixtures of DOX and mPEG-Por conjugate, mPEG-Por 200 μg in 1mL DMSO; (C) UV-vis spectra of mPEG-Por conjugate in water and methanol; (D) fluorescence spectra of DOX/NPs in PBS and methanol, the concentration of DOX/NPs was 20 μg /mL; (E) the fluorescence spectra of DOX/NPs with the addition of methanol, the concentration of DOX/NPs was 200 μg /mL and the volume was 1 mL; (F) the release profile of DOX/NPs in PBS.

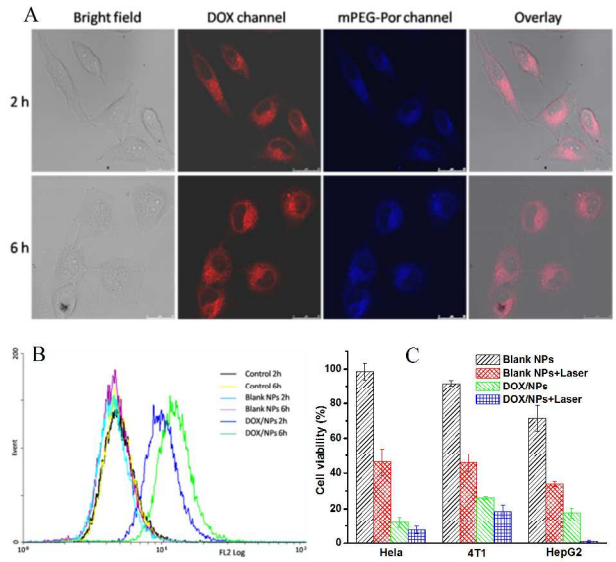

Figure 3. *In vitro* anticancer activity of DOX/NPs, (A) CLSM images of 4T1 cells incubated with DOX/NPs, the concentration of DOX was 8 μg /mL; (B) Flow cytometry of 4T1 cells incubated with DOX/NPs, the concentration of DOX was 8 μg /mL; (C) *in vitro* anticancer activity of DOX/NPs to different cancer cell lines, the concentrations of NPs and DOX/NPs were 80 μg /mL (DOX: 3 μg /mL). HepG2 cell line, p values: blank NPs+laser versus blank NPs, p=0.001; blank NPs versus DOX/NPs, p<0.001; blank NPs versus DOX/NPs+laser, p=0.002; DOX/NPs versus DOX/NPs+laser, p=0.001, Hela cell line, p values: blank NPs+laser versus blank NPs, p=0.006; blank NPs versus DOX/NPs, p<0.001; blank NPs versus DOX/NPs+laser, p=0.013; DOX/NPs versus DOX/NPs+laser, p=0.098; 4T1 cell line, p values: blank NPs+laser versus blank NPs, p=0.003; blank NPs versus DOX/NPs, p<0.001; blank NPs versus DOX/NPs+laser, p=0.034; DOX/NPs versus DOX/NPs+laser, p=0.147, p<0.05 meant significant difference.

The *in vivo* anticancer activity measurement was carried out in breast cancer-bearing Balb/c mice. The growth of tumor was calculated as ratio of tumor volume.[22] After administrated for 20 days, the ratio of volume in saline group was nearly 4. Those in DOX/NPs and blank NPs with laser irradiation groups were 1.9 and 1.7, respectively. In DOX/NPs group, the ratio increased quickly in the first 8 days, it reached the peak of 2.1 at day 10, and then slowly decreased to 1.9 at day 20. The ratio peak in blank NPs with laser irradiation was 2.0 at day 8, and it was slowly reduced to 1.7 at day 20. The DOX/NPs with laser irradiation formula exhibited the best inhibition effect. The peak of the ratio was 1.5 at day 6, it decreased continuously to 1.3 at day 20. All the ratios of tumor volumes in the three groups with therapeutics were all decreased in the late days to reveal effective inhibition of tumor growth. The DOX/NPs with laser irradiation formula exhibited the most efficient anticancer activity *in vivo*. The survival rates of mice bearing tumor after treatments showed the promising therapeutic effect of DOX/NPs (Figure S11).

The body weights of all the mice were stable, the ratios of body weight were within 0.95 to 1.05 (Figure 4C), implying the non-systematic toxicity of the formulas.[23] The tumor tissues administrated with the four formulas were stained by HE (Figure 4D). The tissues were in loose arrangement, multiple patchy necrosis was observed. Gaps were found in the centre of tissues and the ophvacity was increased. There were protein like substances and sporadic cell debris were observed, the contour of blood vessels were destroyed. The tumor administrated with DOX/NPs with laser irradiation was the most seriously damaged, which domenstrated synergistic chemo-photodynamic therapy exhibited the best anticancer activity *in vivo*.

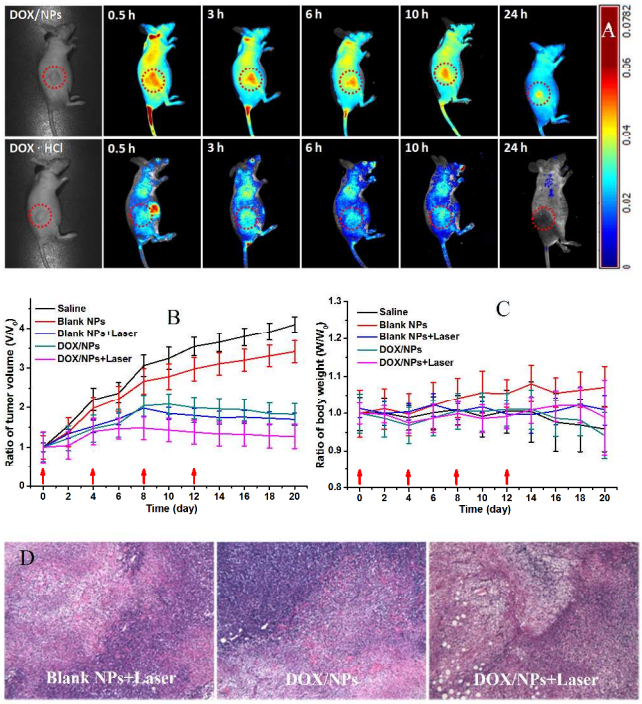

Figure 4. *In vivo* anticancer activity of DOX/NPs, (A) *in vivo* imaging of DOX/NPs administrated tumor-bearing nude mouse; (B) the tumor volumes on the mice administrated with DOX/NPs, p values at 20 days: saline versus blank NPs, p=0.042; saline versus blank NPs+laser, p=0.003; saline versus DOX/NPs, p<0.046; saline versus DOX/NPs+laser, p=0.004; blank NPs versus blank NPs+laser, p<0.001; blank NPs versus DOX/NPs+laser, p=0.092; DOX/NPs versus DOX/NPs+laser, p=0.035, p<0.05 meant significant difference. (C) body weights of mice during therapy, p values at 20 days: saline versus blank NPs, p=0.092; saline versus blank NPs+laser, p=0.845; saline versus DOX/NPs, p=0.994; saline versus DOX/NPs+laser, p=0.375; blank NPs versus blank NPs+laser, p=0.019; blank NPs versus DOX/NPs+laser, p=0.186; DOX/NPs versus DOX/NPs+laser, p=0.295, p<0.05 meant significant difference. (D) HE stained tumor tissues of mice administrated with DOX/NPs (magnification ×100), The DOX dose was 5 mg/kg, the red arrow was the day for injection.

In conclusion, a facile strategy to generate polymeric nanoparticles with synergistic chemo and photodynamic therapy was reported. Photosensitizer tetrakis(4-carboxyphenyl) porphyrin was conjugated to mPEG, the mPEG-Por conjugates were self-assembled into nanoparticles to trap DOX, the π-π stacking interaction between DOX and nanoparticles enhanced the drug loading content dramatically. The DOX/NPs were internalized and aggregated in tumors via EPR effect. The formulation of DOX/NPs with laser irradiation in tumor-bearing mice exhibited efficient anticancer activity both *in vitro* and *in vivo*.

Acknowledgements

This work was funded by NSFC (No. 51222304, 31170921, 51403137), MOE of China (No. 20130181110038, IRT1163), and Sichuan University (2014SCU11015).

Notes and references

National Engineering Research Center for Biomaterials, Sichuan University, 29# Wangjiang Road, Chengdu 610064 China. Fax: 0086-28-85412923; Tel: 0086-28-85412923; E-mail: caojun@scu.edu.cn; bhe@scu.edu.cn

† Electronic Supplementary Information (ESI) available: [details of any supplementary information available should be included here]. See DOI: 10.1039/b000000x/

1. H. Wang, F. Li, C. Du, H. Wang, R. I. Mahato and Y. Huang, *Mol. Pharm.*, 2014, **11**, 2600; H. Wang, Q. Guo, Y. Jiang, E. Liu, Y. Zhao, H. Wang, Y. Li and Y. Huang, *Adv. Funct. Mater.*, 2013, **23**, 6068.
2. Y. Shen, E. Jin, B. Zhang, C. J. Murphy, M. Sui, J. Zhao, J. Wang, J. Tang, M. Fan, E. Van Kirk and W. J. Murdoch, *J. Am. Chem. Soc.*, 2010, **132**, 4259; T. Sun, J. Du, Y. Yao, C. Mao, S. Dou, S. Huang, P. Zhang, K. Leong, E. Song and J. Wang, *ACS Nano*, 2011, **5**, 1483; X. Xiong and A. Lavasanifar, *ACS Nano*, 2011, **5**, 5202; S. Guo, C. Lin, Z. Xu, L. Miao, Y. Wang and L. Huang, *ACS Nano*, 2014, **8**, 4996; M. Zheng, C. Yue, Y. Ma, P. Gong, P. Zhao, C. Zheng, Z. Sheng, P. Zhang, Z. Wang and L. Cai, *ACS Nano*, 2013, **7**, 2056; Z. Sheng, D. Hu, M. Zheng, P. Zhao, H. Liu, D. Gao, P. Gong, G. Gao, P. Zhang, Y. Ma and L. Cai, *ACS Nano*, 2014, **8**, 12310; X. Su, Z. Wang, L. Li, M. Zheng, C. Zheng, P. Gong, P. Zhao, Y. Ma, Q. Tao and L. Cai, *Mol. Pharm.*, 2013, **10**, 1901.
3. D. Dolmans, D. Fukumura and R. K. Jain, *Nat. Rev. Cancer*, 2003, **3**, 380; A. Castano, P. Mroz and M. Hamblin, *Nat. Rev. Cancer*, 2006, **6**, 535.
4. Y. Yuan, J. Liu and B. Liu, *Angew. Chem. Int. Ed.*, 2014, **53**, 7163; C. Lottner, K.-C. Bart, G. Bernhardt and H. Brunner, *J. Med. Chem.*, 2002, **45**, 2064; J. Králová, Z. Kejík, T. Bríza, P. Poucková, A. Král, P. Martásek and V. Král, *J. Med. Chem.*, 2009, **53**, 128.
5. L. Zhang, Y. Lin, Y. Zhang, R. Chen, Z. Zhu, W. Wu and X. Jiang, *Macromol. Biosci.*, 2012, **12**, 83; W. Miao, G. Shim, S. Lee, Y. Choe and Y. Oh, *Biomaterials*, 2013, **34**, 3402; C. Conte, F. Ungaro, G. Maglio, P. Tirino, G. Siracusano, M. Sciortino, N. Leone, G. Palma, A. Barbieri, C. Arra, A. Mazzaglia and F. Quaglia, *J. Control. Release*, 2013, **167**, 40.
6. Z. Liu, J. Robinson, X. Sun and H. Dai, *J. Am. Chem. Soc.*, 2008, **130**, 10876; K. Yang, L. Feng, X. Shi and Z. Liu, *Chem. Soc. Rev.*, 2013, **42**, 530.
7. Q. Zhong, V. Diev, S. Roberts, P. Antunez, R. Brutchey, S. Bradforth and M. Thompson, *ACS Nano*, 2013, **7**, 3466; N. Sahoo, H. Bao, Y. Pan, M. Pal, M. Kakran, H. Cheng, L. Li and L. Tan, *Chem. Comm.*, 2011, **47**, 5235; Y. Pan, H. Bao, N. Sahoo, T. Wu and L. Li, *Adv. Funct. Mater.*, 2011, **21**, 2754.
8. Y. Gao, Y. Kuang, Z. Guo, Z. Guo, I. Krauss and B. Xu, *J. Am. Chem. Soc.*, 2009, **131**, 13576; X. Li, J. Li, Y. Gao, Y. Kuang, J. Shi and B. Xu, *J. Am. Chem. Soc.*, 2010, **132**, 17707.
9. F. Zhao, M. L. Ma and B. Xu, *Chem. Soc. Rev.*, 2009, **38**, 883; M.-R. Lee, K. Baek, H. Jin, Y. Jung and I. Shin, *Angew. Chem. Int. Ed.*, 2004, **43**, 1675.
10. M. Elsabahy and K. L. Wooley, *Chem. Soc. Rev.*, 2012, **41**, 2545; K. Soppimath, T. Aminabhavi, A. Kulkarni and W. Rudzinski, *J. Control. Release*, 2001, **70**, 1.
11. N. Li, Q. Yi, K. Luo, C. Guo, D. Pan and Z. Gu, *Biomaterials*, 2014, **35**, 9529; Z. Yu, R. M. Schmaltz, T. Bozeman, R. Paul, M. Rishel, K. Tsosie and S. Hecht, *J. Am. Chem. Soc.*, 2013, **135**, 2883; B. Schroeder, M. Ghare, C. Bhattacharya, R. Paul, Z. Yu, P. Zaleski, T. Bozeman, M. Rishel and S. Hecht, *J. Am. Chem. Soc.*, 2014, **136**, 13641; H. Gao, Q. Zhang, Z. Yu, Q. He, *Cur. pharm biotech.,* 2014,**15**, 210.
12. C. Peng, P. Lai, F. Lin, S. Yueh-Hsiu Wu and M. Shieh, *Biomaterials*, 2009, **30**, 3614.
13. Y. Zhou and D. Yan, *Angew. Chem. Int. Ed.*, 2004, **43**, 4896.
14. E. Rabani, D. Reichman, P. Geissler and L. Brus, *Nature*, 2003, **426**, 271; D. Shi, M. Matsusaki and M. Akashi, *J. Control. Release*, 2011, **149**, 182.
15. M. Wilhelm, C. Zhao, Y. Wang, R. Xu, M. Winnik, J. Mura, G. Riess and M. Croucher, *Macromolecules*, 1991, **24**, 1033; S. Kwon, J. Park, H. Chung, I. Kwon, S. Jeong and I. Kim, *Langmuir*, 2003, **19**, 10188.
16. J. Du, L. Tang, W. Song, Y. Shi and J. Wang, *Biomacromolecules*, 2009, **10**, 2169; J.Tan, S. Kim, F. Nederberg, K. Fukushima, D. Coady, A. Nelson, Y.Yang and J. Hedrick, *Macromol. Rapid Comm.*, 2010, **31**, 1187; S. Li, W. Wu, K. Xiu, F. Xu, Z. Li and J. Li, *J. Biomed. Nanotech.*, 2014, **10**, 1480; M. Lee, J. Jeong and D. Kim, *Biomacromolecules*, 2014, **16**, 136; A. Di Martino and V. Sedlarik, *Int.Pharm.*, 2014, **474**, 134.
17. F. Li, Y. Zhu, B. You, D. Zhao, Q. Ruan, Y. Zeng and C. Ding, *Adv. Funct. Mater.*, 2010, **20**, 669; A. Smith, R. Williams, C. Tang, P. Coppo, R. Collins, M. Turner, A. Saiani and R. Ulijn, *Adv. Mater.*, 2008, **20**, 37.
18. Z. Liu, X. Sun, N. Nakayama-Ratchford and H. Dai, *ACS Nano*, 2007, **1**, 50.
19. G. Romero, Y. Qiu, R. A. Murray and S. E. Moya, *Macromol. Biosci.*, 2013, **13**, 234; J.Chen and W. Wu, *Macromol. Biosci.*, 2013, **13**, 623.
20. H. Huang, Q. Yuan, J. Shah and R. Misra, *Adv. Drug Deliv. Rev.*, 2011, **63**, 1332.
21. Y. Matsumura and H. Maeda, *Cancer Res.*, 1986, **46**, 6387; H. Maeda, *Biocon. Chem.*, 2010, **21**, 797.
22. C. Menon, G. Polin, I. Prabakaran, A. Hsi, C. Cheung, J. Culver, J. Pingpank, C. Sehgal, A. Yodh, D. Buerk and D. Fraker, *Cancer Res.*, 2003, **63**, 7232.
23. M. Schipper, N. Nakayama-Ratchford, C. Davis, N. Kam, P. Chu, Z. Liu, X. Sun, H. Dai and S. Gambhir, *Nat. Nano.*, 2008, **3**, 216; Y. Chen, H. Chen and J. Shi, *Adv. Mater.*, 2013, **25**, 3144.